HOKKAIDO UNIVERSITY

Title	Direct imaging of nanogap-mode plasmon-resonant fields
Author(s)	Tanaka, Yoshito; Ishiguro, Hiroyasu; Fujiwara, Hideki et al.
Citation	Optics Express, 19(8), 7726-7733 https://doi.org/10.1364/OE.19.007726
Issue Date	2011-04-11
Doc URL	https://hdl.handle.net/2115/45510
Rights	©2011 Optical Society of America
Type	journal article
File Information	OE19-8_7726-7733.pdf

Hokkaido University Collection of Scholarly and Academic Papers : HUSCAP

Direct imaging of nanogap-mode plasmon-resonant fields

Yoshito Tanaka,[1] Hiroyasu Ishiguro,[1] Hideki Fujiwara,[1,2] Yukie Yokota,[1] Kosei Ueno,[1,2] Hiroaki Misawa,[1] and Keiji Sasaki[1,*]

[1] Research Institute for Electronic Science, Hokkaido University, Sapporo 001-0020, Japan
[2]PRESTO, Japan Science and Technology Agency, Sapporo 001-0020, Japan
**sasaki@es.hokudai.ac.jp*

Abstract: We perform direct local-field imaging of a plasmon-resonant gold nanoparticle pair separated by a gap of several nanometers using a scattering-type near-field optical microscope with a sharp silicon tip of atomic force microscope. The sharp tip allows the access for the nanogap and the high spatial resolution. Our results provide experimental evidence that the nanogap structure produces an optical spot with the size of a single nanometer (< 10 nm). This is not only of fundamental importance in the field of nanophotonics, but also provide significant information for the development of plasmonic devices with the nanogap structures.

©2011 Optical Society of America

OCIS codes: (220.4241) Nanostructure fabrication; (250.5403) Plasmonics; (180.4243) Near-field microscopy; (240.6680) Surface plasmons.

References and links

1. S. A. Maier, P. G. Kik, H. A. Atwater, S. Meltzer, E. Harel, B. E. Koel, and A. A. G. Requicha, "Local detection of electromagnetic energy transport below the diffraction limit in metal nanoparticle plasmon waveguides," Nat. Mater. **2**(4), 229–232 (2003).
2. L. Feng, D. Van Orden, M. Abashin, Q. J. Wang, Y. F. Chen, V. Lomakin, and Y. Fainman, "Nanoscale optical field localization by resonantly focused plasmons," Opt. Express **17**(6), 4824–4832 (2009).
3. J. A. Schuller, E. S. Barnard, W. Cai, Y. C. Jun, J. S. White, and M. L. Brongersma, "Plasmonics for extreme light concentration and manipulation," Nat. Mater. **9**(3), 193–204 (2010).
4. M. L. Brongersma and P. G. Kik, *Surface Plasmon Nanophotonics* (Springer, Dordrecht, 2007).
5. S. Kühn, U. Håkanson, L. Rogobete, and V. Sandoghdar, "Enhancement of single-molecule fluorescence using a gold nanoparticle as an optical nanoantenna," Phys. Rev. Lett. **97**(1), 017402 (2006).
6. P. Mühlschlegel, H.-J. Eisler, O. J. F. Martin, B. Hecht, and D. W. Pohl, "Resonant optical antennas," Science **308**(5728), 1607–1609 (2005).
7. H. Fischer and O. J. F. Martin, "Engineering the optical response of plasmonic nanoantennas," Opt. Express **16**(12), 9144–9154 (2008).
8. W. Srituravanich, N. Fang, C. Sun, Q. Luo, and X. Zhang, "Plasmonic Nanolithography," Nano Lett. **4**(6), 1085–1088 (2004).
9. T. H. Taminiau, F. D. Stefani, F. B. Segerink, and N. F. Van Hulst, "Optical antennas direct single-molecule emission," Nat. Photonics **2**(4), 234–237 (2008).
10. A. N. Grigorenko, N. W. Roberts, M. R. Dickinson, and Y. Zhang, "Nanometric optical tweezers based on nanostructured substrates," Nat. Photonics **2**(6), 365–370 (2008).
11. M. Inoue and K. Ohtaka, "Surface Enhanced Raman Scattering by Metal Spheres. I. Cluster Effect," J. Phys. Soc. Jpn. **52**(11), 3853–3864 (1983).
12. H. Xu, J. Aizpurua, M. Käll, and P. Apell, "Electromagnetic contributions to single-molecule sensitivity in surface-enhanced raman scattering," Phys. Rev. E Stat. Phys. Plasmas Fluids Relat. Interdiscip. Topics **62**(3 3 Pt B), 4318–4324 (2000).
13. E. Hao and G. C. Schatz, "Electromagnetic fields around silver nanoparticles and dimers," J. Chem. Phys. **120**(1), 357–366 (2004).
14. H. Xu, E. J. Bjerneld, M. Käll, and L. Borjesson, "Spectroscopy of single hemoglobin molecules by surface enhanced Raman scattering," Phys. Rev. Lett. **83**(21), 4357–4360 (1999).
15. K. Ueno, S. Juodkazis, T. Shibuya, Y. Yokota, V. Mizeikis, K. Sasaki, and H. Misawa, "Nanoparticle plasmon-assisted two-photon polymerization induced by incoherent excitation source," J. Am. Chem. Soc. **130**(22), 6928–6929 (2008).
16. H. Xu and M. Käll, "Surface-plasmon-enhanced optical forces in silver nanoaggregates," Phys. Rev. Lett. **89**(24), 246802 (2002).
17. K. Ueno, S. Juodkazis, T. Shibuya, Y. Yokota, V. Mizeikis, K. Sasaki, and H. Misawa, "Nanoparticle-enhanced photopolymerization," J. Phys. Chem. C **113**(27), 11720–11724 (2009).

#142490 - $15.00 USD Received 10 Feb 2011; revised 10 Mar 2011; accepted 29 Mar 2011; published 6 Apr 2011
(C) 2011 OSA

18. K. Imura, H. Okamoto, M. K. Hossain, and M. Kitajima, "Visualization of localized intense optical fields in single gold-nanoparticle assemblies and ultrasensitive Raman active sites," Nano Lett. **6**(10), 2173–2176 (2006).
19. R. Hillenbrand, F. Keilmann, P. Hanarp, D. S. Sutherland, and J. Aizpurua, "Coherent imaging of nanoscale plasmon patterns with a carbon nanotube optical probe," Appl. Phys. Lett. **83**(2), 368–370 (2003).
20. Y.-K. Kim, J. B. Ketterson, and D. J. Morgan, "Scanning plasmon optical microscope operation in atomic force microscope mode," Opt. Lett. **21**(3), 165–167 (1996).
21. Z. H. Kim and S. R. Leone, "Polarization-selective mapping of near-field intensity and phase around gold nanoparticles using apertureless near-field microscopy," Opt. Express **16**(3), 1733–1741 (2008).
22. R. Esteban, R. Vogelgesang, J. Dorfmüller, A. Dmitriev, C. Rockstuhl, C. Etrich, and K. Kern, "Direct near-field optical imaging of higher order plasmonic resonances," Nano Lett. **8**(10), 3155–3159 (2008).
23. R. Hillenbrand and F. Keilmann, "Optical oscillation modes of plasmon particles observed in direct space by phase-contrast near-field microscopy," Appl. Phys. B **73**, 239–243 (2001).
24. R. L. Olmon, P. M. Krenz, A. C. Jones, G. D. Boreman, and M. B. Raschke, "Near-field imaging of optical antenna modes in the mid-infrared," Opt. Express **16**(25), 20295–20305 (2008).
25. M. Schnell, A. Garcia-Etxarri, J. Alkorta, J. Aizpurua, and R. Hillenbrand, "Phase-resolved mapping of the near-field vector and polarization state in nanoscale antenna gaps," Nano Lett. **10**(9), 3524–3528 (2010).
26. E. Cubukcu, E. A. Kort, K. B. Crozier, and F. Capasso, "Plasmonic laser antenna," Appl. Phys. Lett. **89**(9), 093120 (2006).
27. N. F. Yu, E. Cubukcu, L. Diehl, D. Bour, S. Corzine, J. T. Zhu, G. Höfler, K. B. Crozier, and F. Capasso, "Bowtie plasmonic quantum cascade laser antenna," Opt. Express **15**(20), 13272–13281 (2007).
28. D.-S. Kim, J. Heo, S.-H. Ahn, S. W. Han, W. S. Yun, and Z. H. Kim, "Real-space mapping of the strongly coupled plasmons of nanoparticle dimers," Nano Lett. **9**(10), 3619–3625 (2009).
29. M. Rang, A. C. Jones, F. Zhou, Z. Y. Li, B. J. Wiley, Y. N. Xia, and M. B. Raschke, "Optical near-field mapping of plasmonic nanoprisms," Nano Lett. **8**(10), 3357–3363 (2008).
30. The images were supplied by *NANOSENSORS* (www.nanosensors.com).
31. H. Fujiwara, Y. Tanaka, H. Ishiguro, A. Saito, and K. Sasaki, "Direct observation of localized fields in nanogaps between metal particles," Appl. Phys. Express **2**(10), 102002 (2009).
32. B. D. Mangum, C. Mu, and J. M. Gerton, "Resolving single fluorophores within dense ensembles: contrast limits of tip-enhanced fluorescence microscopy," Opt. Express **16**(9), 6183–6193 (2008).
33. P. G. Gucciardi, G. Bachelier, and M. Allegrini, "Far-field background suppression in tip-modulated apertureless near-field optical microscopy," J. Appl. Phys. **99**(12), 124309 (2006).
34. B. Knoll and F. Keilmann, "Electromagnetic fields in the cutoff regime of tapered metallic waveguides," Opt. Commun. **162**(4-6), 177–181 (1999).
35. Y. Inouye and S. Kawata, "Near-field scanning optical microscope with a metallic probe tip," Opt. Lett. **19**(3), 159–161 (1994).

Localized surface plasmons (LSPs) of metal nanoparticles and engineered nanostructures have attracted much attention as an approach to overcome the optical diffraction limit [1–4]. They work as effective nanoantennas in the visible and infrared wavelength range due to the optical excitation of LSPs [5–7], which can efficiently convert propagating light into nanoscale-confined and strongly enhanced optical fields. This downscaling from the diffraction limit to the nanometer dimension is a key element in the development of noble optics and photonics, including optical nanolithography [8], nanoscale optical microscopy [9], and nanometric optical tweezers [10].

It has been widely shown that the size, shape, and structure of the nanoantennas determine their optical characteristics, including resonant frequencies, local-field distributions, and field enhancements [12,13]. In particular, many calculations have suggested that plasmon-resonant nanoantennas composed of a pair of metal nanoparticles with a gap below 10 nm ("nanogap") produce an intense optical spot that is about two orders of magnitude smaller than the wavelength of the light. This effect is understood as the result of the strong coupling of plasmons between the nanoparticles [7,11–13]. Nanogap antennas have led to the wide range of physically interesting and technologically important phenomena, such as single-molecule surface-enhanced Raman scattering [14], nonlinear photochemical reactions induced by an incoherent excitation source [15], and optical trapping of single molecules [16]. For the understanding of these nanogap-induced phenomena and the applications in nanooptics and nanophotonics, it is important to determine the spatial characteristics of the photon localization within the nanogap experimentally with a single nanometer resolution. Unfortunately, such experiment remains as a challenging task.

A few techniques have been used to observe the local-field distribution within the nanogap. In a previous work [15,17], a photopolymerization process was exploited for the near-field imaging of nanogap antennas; in this process, the intensity distributions are

#142490 - $15.00 USD Received 10 Feb 2011; revised 10 Mar 2011; accepted 29 Mar 2011; published 6 Apr 2011
(C) 2011 OSA

recorded on photoresist films. However, this near-field photochemical imaging technique is not a direct optical-field measurement but rather is mediated by multiple chemical reaction processes; as a result, the recorded photoproducts may not reflect the precise local-field distribution. Another promising technique is near-field scanning optical microscopy (NSOM). In this technique, an aperture-type NSOM is used to illustrate that the electric field is confined at an interstitial site in the gold particle pairs [18]. The spatial resolution, which is restricted by the aperture size of the metal-coated optical-fiber probe, is typically 50-100 nm. However, this resolution is insufficient for the precise observation of a tiny optical spot on the nanogap antenna, for which single nanometer-scale imaging is required. A scattering-type NSOM has been also widely used for the plasmonic local-field imaging [19–29]. This technique demonstrates that a dimer antenna produces the localized field within a gap of several tens of nanometers [26,27]. Furthermore, the local-field distributions of a gold nanocube pair separated by the nanogap were mapped with the high spatial resolution (~20 nm from the full width at half maximum (FWHM) of the intensity maps) and their maps revealed antisymmetric plasmon modes that are different from a simple superposition of two monometric dipole plasmons [28]. However, the visualization of the strong fields within the nanogap was not achieved because of the experimental limitation that the probe tip could not fully access the nanogap area between the nanoparticles. In this paper, we demonstrate the direct observation of nanogap-mode plasmon-resonant fields using a scattering-type NSOM with a very sharp silicon tip of atomic force microscope (AFM). Our results provide experimental evidence that the nanogap antenna generates an optical spot with the size of a single nanometer (< 10 nm).

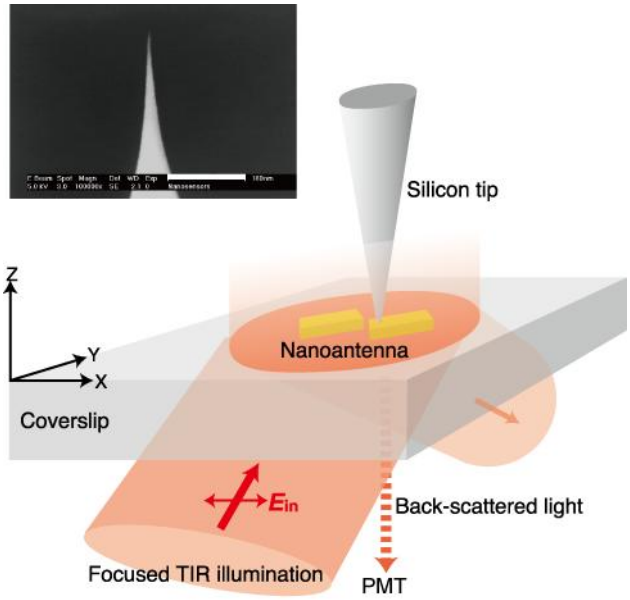

Fig. 1. Direct near-field imaging of optical nanoantennas with a scattering-type NSOM. The nanoantennas are illuminated under the focused TIR conditions. The confined plasmonic fields are scattered by the sharp AFM tip and transformed to propagating waves during the scanning operation. The near-field and the topography images are obtained simultaneously. The inset shows SEM image of the AFM tip apex [30]. Bar = 180 nm.

The schematic of the scattering-type NSOM is shown in Fig. 1 [31]. The extremely sharp AFM tip was used to probe the nanoantennas. The samples were illuminated with laser light at the wavelength of 800 nm under a focused total internal reflection (TIR). Therefore, both topographic and scattered near-field images can be obtained simultaneously. A continuous-wave Ti:sapphire laser beam (wavelength = 800 nm, linewidth = 100 kHz) was used for surface plasmon excitation. The linearly polarized beam was introduced into an inverted

#142490 - $15.00 USD Received 10 Feb 2011; revised 10 Mar 2011; accepted 29 Mar 2011; published 6 Apr 2011
(C) 2011 OSA

optical microscope and was focused by an oil-immersion objective (100 × , numerical aperture = 1.35). A section of the focused beam with the incident angle smaller than the critical angle was masked by a knife edge at the pupil plane of the imaging system; therefore, the sample was illuminated under the focused TIR condition (spot area = 1.2 × 1.7 μm). The TIR illumination technique prevents from being directly heated by the transmitted laser light and greatly reduces the signal background [20,32]. The laser beam was polarized in the parallel direction to the sample surface, i.e., s-polarization along the X-direction in Fig. 1. This polarization could efficiently excite the nanogap-mode plasmon of the dimer nanoantennas. An AFM was placed on the sample stage, and the silicon probe tip was driven at the resonant frequency of the AFM probe. Back-scattered light from the tip was collected by the same objective and detected by a photomultiplier tube (PMT) with a pinhole. This detection configuration allows the efficient measurement of in-plane near-field component (parallel to the sample surface) compared with the vertical component E_z along the Z-direction in Figure. 1. The in-plane component E_x along the X-direction is dominant in the plasmonic fields within the nanogap [25]. The detected signal was demodulated at the second harmonic (~700 kHz) of the resonant frequency of the AFM probe by a lock-in amplifier, which can suppress the scattered light signal from the probe shaft and the sample [32,33]. We note that the out put of the lock-in amplifer is proportional to the near-field amplitude rather than its intensity due to the interference between the scattered near-field and the far-field background [34].

The metal-coated AFM probe tips, which are normally used in the conventional scattering-type NSOMs [21–28,35], can greatly improve the scattered near-field signal. However, the metal-coated tips also restrict the spatial resolution to ~20 nm and limit the access into the gap of single nanometer-scale antennas. Therefore, we chose bare silicon AFM probe tips (SSS-NCH Nanosensors from NanoWorld AG (Switzerland)) that feature a very small tip radius of curvature (typically 2 nm) and a high aspect ratio near the apex (full cone angle < 8° at the 50 nm of the pointed end of the tip). Compared to the metal-coated tips, the perturbation in the local-field distribution for the silicon tip was minified because plasmon resonances at visible wavelengths for the silicon tips are not significant.

The AFM topography and the scattered near-field images for a single 50-nm gold nanosphere are shown in Figs. 2A and 2B. The nanosphere produces two optical lobes of ~15 nm around both ends along the incident polarization direction (Figs. 2B and 2C). The characteristic represents dipolar near-field distribution and agrees well with the numerical calculation in Fig. 2D. This result demonstrates that our scattering-type NSOM using the sharp silicon AFM tips allows for reliable observation of antenna near-field modes with improved spatial resolution compared to the conventional near-field microscopy [21–29].

#142490 - $15.00 USD Received 10 Feb 2011; revised 10 Mar 2011; accepted 29 Mar 2011; published 6 Apr 2011
(C) 2011 OSA

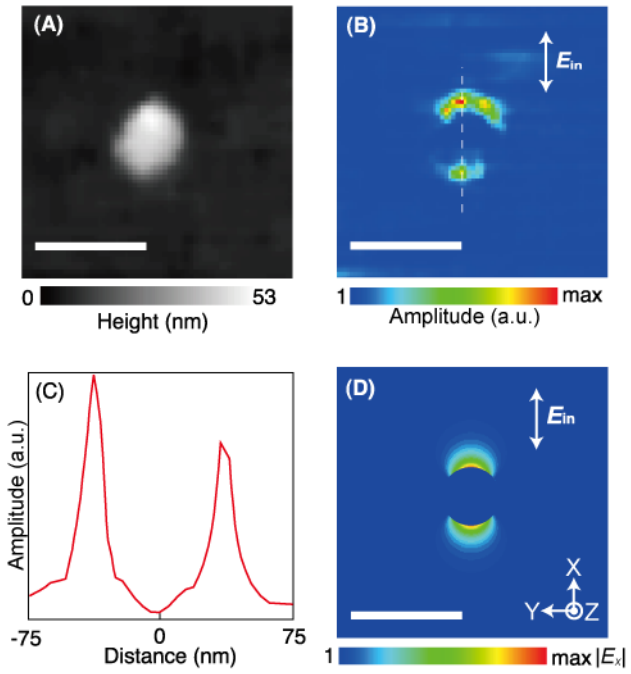

Fig. 2. Near-field image of a simple dipole nanoantenna. Topography (A) and corresponding scattered near-field images (B) of a single gold nanosphere. (C) Line profile along the dashed line marked in (B). FWHM of the two peaks are 15.8 nm and 14.2 nm. (D) Calculated near-field distribution of a 50-nm nanosphere with the same excitation as in (B). The image shows the X-component of the electric field in a height of 25 nm above the substrate. Arrows indicate the polarization directions of the incident probe beam. Bar = 100 nm.

A dimer nanoantenna composed of a pair of diagonally aligned gold nanoblocks with nanogap is shown in the scanning electron microscope (SEM) image of Fig. 3A. The dimer was fabricated on a glass substrate using electron beam lithography and lift-off techniques. The fabrication procedure is described in earlier reports [15,17]. The gap distance of ~7 nm allowed the AFM probe tip to access the bottom of the nanogap. The block dimension of 115 × 115 × 30 nm was chosen so that the far-field resonance is close to the incident wavelength of 800 nm (see the scattering spectrum in Fig. 3B). The calculated near-field distribution of the nanogap model based on the geometry of Fig. 3A is shown in Fig. 3C. The excitation conditions were also chosen as in the experiments; more specifically, an s-polarized plane wave at a wavelength of 800 nm illuminates the antennas on the glass substrate at an incidence angle of 60° under TIR condition, as shown in Fig. 1. The distribution predicts the presence on optical spot in single nanometer size inside the nanogap. Moreover, the theoretical scattering spectrum of the nanogap model (Fig. 3D) is in good agreement with the experimental data in Fig. 3B.

#142490 - $15.00 USD Received 10 Feb 2011; revised 10 Mar 2011; accepted 29 Mar 2011; published 6 Apr 2011
(C) 2011 OSA

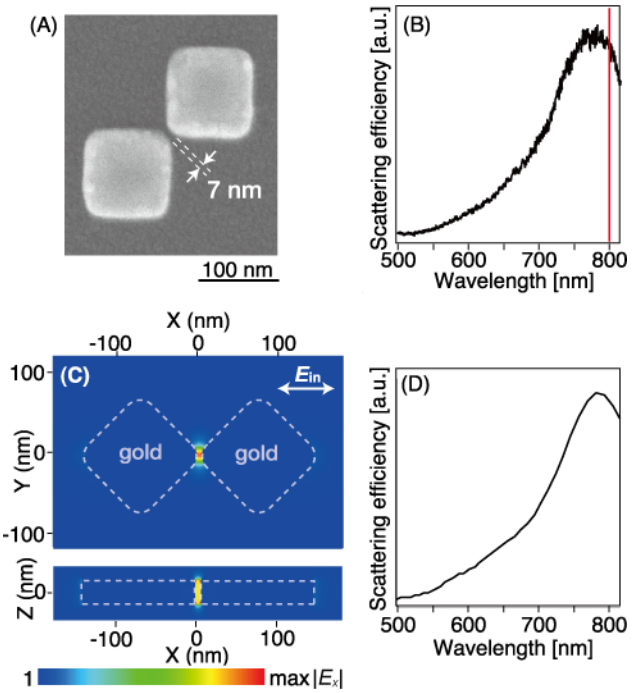

Fig. 3. Dimer nanoantenna with a single nanometer-scale gap. SEM image (A) and experimental scattering spectrum (B) of a single pair of diagonally aligned gold nanoblocks, with an interparticle edge-to-edge separation distance of ~7 nm. The scattering spectrum (B) is normalized by the incident white light intensity. The vertical red line in (B) represents the incident beam wavelength. (C) Calculated near-field distributions of a model gold nanogap antenna; block size = 115 × 115 × 30 nm, curvature radius of each corner = 20 nm, and gap distance = 7 nm. The images show the X- component of the electric field in the X-Y plane at half-height and the X-Z plane along the diagonal line of the antenna. (D) Theoretical scattering spectrum of the same model nanogap antenna as in (C). In the experimental and theoretical scattering spectra, the optical excitation is polarized along the dimer axis.

Figures 4A and 4B show the topography and the corresponding scattered near-field images, respectively, for the nanogap shown in Fig. 3A. An intense scattered near-field signal from the probe tip was observed in the nanogap area, and its magnitude was at a maximum in the narrowest gap. For this measurement, the AFM tip fully accessed the nanogap area between the two blocks, as shown in the topography line-profile in Fig. 4C. From the near-field image and profile in Figs. 4B and 4C, respectively, it can be clearly seen that the nanogap generates a single elliptical nanospot with strength considerably stronger than that of the side spots at the outer ends of the dimer nanoantenna, which corresponds to the theoretical prediction. This nanospot was obtained with high reproducibility for five repeated measurements, and the FWHMs of the nanogap-mode plasmonic field distribution were 9.2 ± 0.5 nm in the dimer axis direction and 12.6 ± 0.8 nm in the perpendicular direction (Figs. 4C and 4D). In this determination of the spot size along the dimer axis, the influence of z-direction motion of the scanning probes was not considered. Our results represent the first experiment in which the nanogap-mode plasmon-resonant fields were directly observed on the single nanometer scale. In addition, we confirmed that the intense fields within the nanogap become negligibly weak when the incident polarization is rotated by 90° (Fig. 4E), i.e., p-polarization, as expected theoretically. These results also support our previous reports on the nanogap-mode plasmon-induced polymerization [15,17].

#142490 - $15.00 USD Received 10 Feb 2011; revised 10 Mar 2011; accepted 29 Mar 2011; published 6 Apr 2011
(C) 2011 OSA

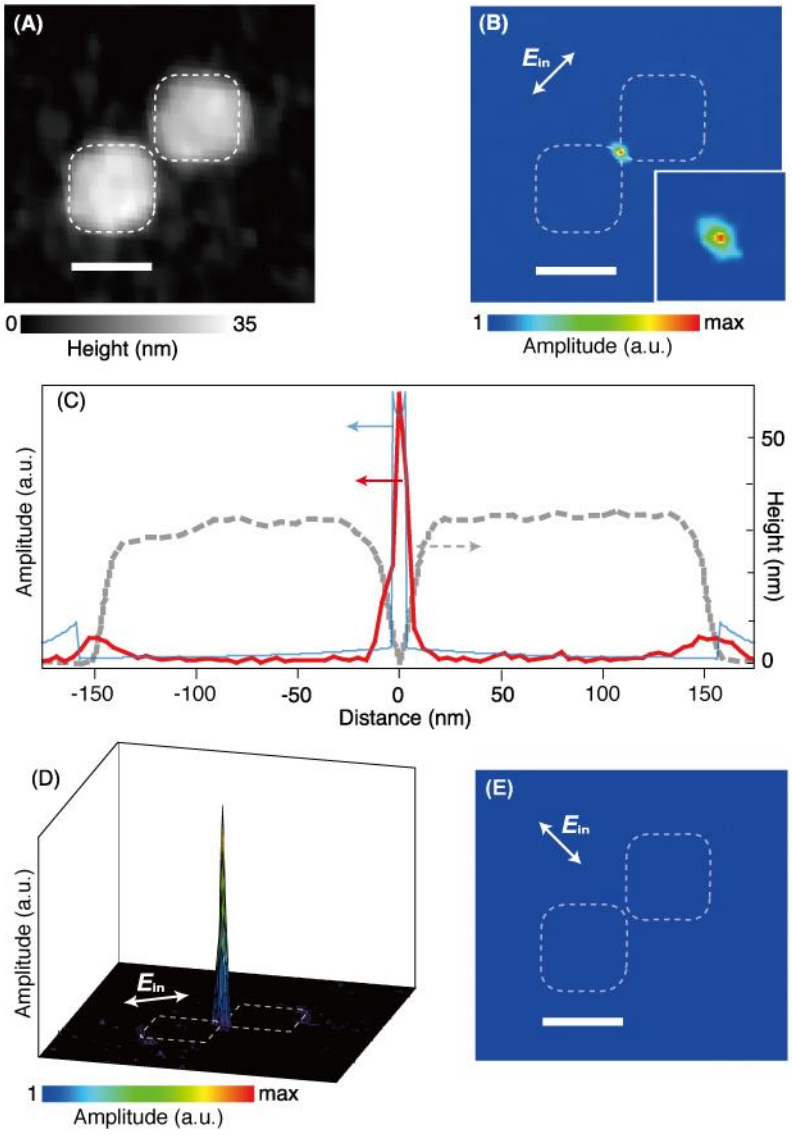

Fig. 4. Near-field image of the nanogap plasmon mode. Topography (A) and corresponding scattered near-field images (B) of the nanogap antenna in Fig. 3. The two dashed squares in (B) spatially correspond to the ones in (A). The inset in (B) shows the 2x magnified view around the interparticle gap area. (C) Line profiles of the topography (gray dotted curve) and the near-field (red solid curve) images along the dimer axis in (A) and (B), respectively. The blue solid curve shows a line profile of the calculated near-field image (top of Fig. 3C) along the dimer axis. The FWHM of the measured near-field distributions is 9.2 ± 0.5 nm from five repeated measurements. (D) A 3-D view of the near-field image in (B). (E) Scattered near-field image of the antenna with the polarization direction perpendicular to the dimer axis. The color scale is same as in (B). Bar = 100 nm.

In conclusion, the direct imaging of nanogap-mode plasmon-resonant fields provides experimental evidence that the nanogap antenna produces a single nanometer-scale optical spot. This result will have a fundamental impact on the field of nanophotonics and promises

#142490 - $15.00 USD Received 10 Feb 2011; revised 10 Mar 2011; accepted 29 Mar 2011; published 6 Apr 2011
(C) 2011 OSA

potential applications of nanogap antennas, including optical imaging, optical spectroscopy, optical lithography, optical data storage, and optical manipulation.

Acknowledgement

The present work was partly supported by the Ministry of Education, Culture, Sports, Science, and Technology of Japan: KAKENHI Grant-in-Aid for Scientific Research on the Priority Area "Strong Photon-Molecule Coupling Fields" (No. 470, 1904900209) and for Young Scientists (B) (2171009009) to Yoshito Tanaka.

#142490 - $15.00 USD Received 10 Feb 2011; revised 10 Mar 2011; accepted 29 Mar 2011; published 6 Apr 2011
(C) 2011 OSA